1
Mass Analysis

Gene Hart-Smith and Stephen J. Blanksby

1.1
Introduction

Modern day mass analyzer technologies have, together with soft ionization techniques, opened powerful new avenues by which insights can be gained into polymer systems using mass spectrometry (MS). Recent years have seen important advances in mass analyzer design, and a suite of effective mass analysis options are currently available to the polymer chemist. In assessing the suitability of different mass analyzers toward the examination of a given polymer sample, a range of factors, ultimately driven by the scientific questions being pursued, must be taken into account. It is the aim of the current chapter to provide a reference point for making such assessments.

The chapter will open with a summary of the measures of mass analyzer performance most pertinent to polymer chemists (Section 1.2). How these measures of performance are defined and how they commonly relate to the outcomes of polymer analyses will be presented. Following this, the various mass analyzer technologies of most relevance to contemporary MS will be discussed (Section 1.3); basic operating principles will be introduced, and the measures of performance described in Section 1.2 will be summarized for each of these technologies. Finally, an instrument's tandem and multiple-stage MS (MS/MS and MS^n, respectively) capabilities can play a significant role in its applicability to a given polymer system. The capabilities of different mass analyzers and hybrid mass spectrometers in relation to these different modes of analysis will be summarized in Section 1.4.

1.2
Measures of Performance

When judging the suitability of a given mass analyzer toward the investigation of a polymer system, the relevant performance characteristics will depend on the scientific motivations driving the study. In most instances, knowledge of the following measures of mass analyzer performance will allow a reliable assessment to be made: mass resolving power, mass accuracy, mass range, linear dynamic range, and abundance

Mass Spectrometry in Polymer Chemistry, First Edition.
Edited by Christopher Barner-Kowollik, Till Gruendling, Jana Falkenhagen, and Steffen Weidner

sensitivity. How these different performance characteristics are defined, and how they relate to the data collected from polymer samples is expanded upon in the sections below.

1.2.1 Mass Resolving Power

Mass analyzers separate gas-phase ions based on their mass-to-charge ratios (m/z); how well these separations can be performed and measured is defined by the instrument's mass resolving power. IUPAC recommendations allow for two definitions of mass resolving power [1]. The "10% valley definition" states that, for two singly charged ion signals of equal height in a mass spectrum at masses M and $(M - \Delta M)$ separated by a valley which, at its lowest point, is 10% of the height of either peak, mass resolving power is defined as $M/\Delta M$. This definition of mass resolving power is illustrated in portion A of Figure 1.1. The "peak width definition" also defines mass resolving power as $M/\Delta M$; in this definition, M

$$\text{mass resolving power} = \frac{M}{\Delta M}$$

(A) 10 percent valley definition

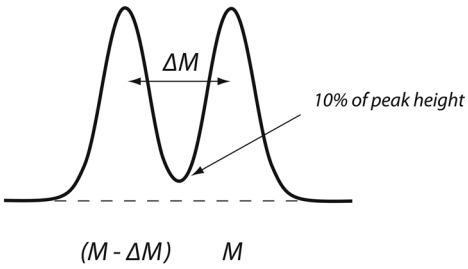

(B) FWHM definition

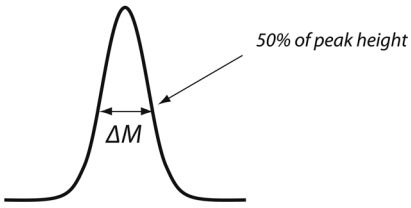

Figure 1.1 Methods of calculating mass resolving power. Portion (A) illustrates calculation via the 10% valley definition. Portion (B) illustrates calculation via the FWHM definition.

refers to the mass of singly charged ions that make up a single peak, and ΔM refers to the width of this peak at a height which is a specified fraction of the maximum peak height. It is recommended that one of three specified fractions should always be used: 50%, 5%, or 0.5%. In practice, the value of 50% is frequently utilized; this common standard, illustrated in portion B of Figure 1.1, is termed the "full width at half maximum height" (FWHM) definition. The mass resolving power values quoted for the mass analyzers described in this chapter use the FWHM criterion.

In the context of polymer analysis, the mass resolving power is important when characterizing different analyte ions of similar but nonidentical masses. These different ions may contain separate vital pieces of information. An example of this would be if the analytes of interest contain different chain end group functionalities; characterization of these distinct end groups would allow separate insights to be gained into polymer formation processes. Whether or not this information can be extracted from the mass spectrum depends on the resolving power of the mass analyzer. The importance of mass resolving power in this context has been illustrated in Figure 1.2 using data taken from a study conducted by Szablan *et al.*, who were interested in the reactivities of primary and secondary radicals derived from various photoinitiators [2]. Through the use of a 3D ion trap mass analyzer, these authors were able to identify at least 14 different polymer end group combinations within a m/z window of 65. This allowed various different initiating radical fragments to be identified, and insights to be gained into the modes of termination that were taking place in these polymerization systems. It can be seen that the mass resolving power of the 3D ion trap allowed polymer structures differing in mass by 2 Da to be comfortably distinguished from one another.

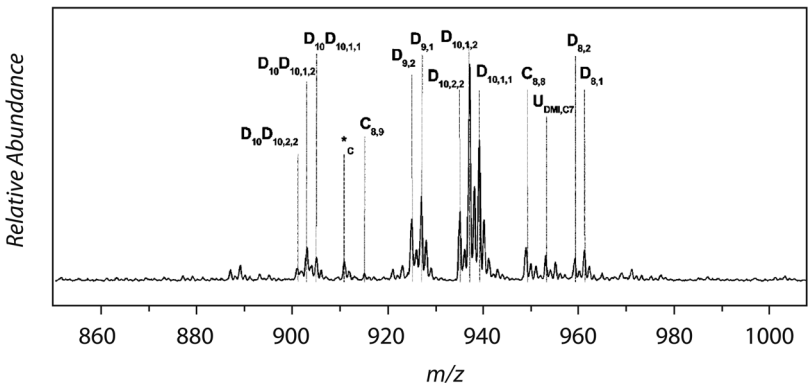

Figure 1.2 A 3D ion trap-derived mass spectrum of the polymer obtained from an Irgacure 819-initiated pulsed laser polymerization of dimethyl itaconate, adapted from Figure 12 of Szablan *et al.* [2].

1.2.2
Mass Accuracy

Mass accuracy refers to the m/z measurement error – that is, the difference between the true m/z and the measured m/z of a given ion – divided by the true m/z of the ion, and is usually quoted in terms of parts per million (ppm). For a single reading, the term "mass measurement error" may be used [3]. It is usual for mass accuracy to increase with mass resolving power, and a higher mass accuracy increases the degree of confidence in which peak assignments can be made based upon the m/z. This lies in the fact that increases in mass accuracy will result in an increased likelihood of uniquely identifying the elemental compositions of observed ions.

When attempting to identify peaks in mass spectra obtained from a polymer sample, it is common for different feasible analyte ions to have similar but non-isobaric masses. If the theoretical m/z's of these potential ion assignments differ by an amount lower than the expected mass accuracy of the mass analyzer, an ion assignment cannot be made based on m/z alone. Ideally such a scenario would be resolved through complementary experiments using, for example, MS/MS or alternate analytical techniques, in which one potential ion assignment is confirmed and the others are rejected. However if such methods are not practical, the use of a mass analyzer capable of greater mass accuracy may be necessary. An example of the use of ultrahigh mass accuracy data for this purpose can be found in research conducted by Gruendling *et al.*, who were investigating the degradation of reversible addition-fragmentation chain transfer (RAFT) agent-derived polymer end groups [4]. These authors initially used a 3D ion trap instrument to identify a peak at m/z 1275.6 for which three possible degradation products could be assigned. To resolve this issue, the same sample was analyzed using a Fourier transform ion cyclotron resonance (FT-ICR) mass analyzer. As illustrated in Figure 1.3, the ultrahigh mass accuracy obtained using FT-ICR allowed two of the potential ion assignments to be

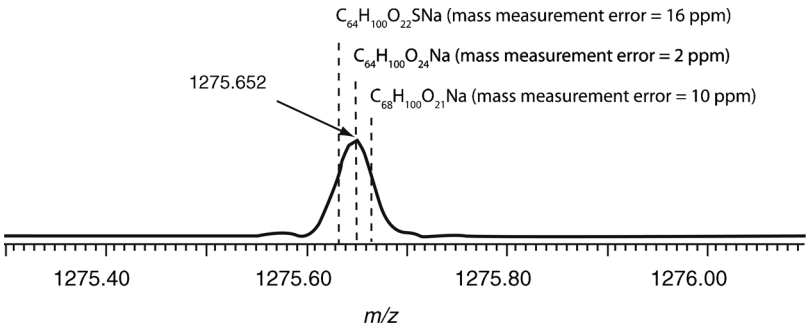

Figure 1.3 An FT-ICR-derived signal from the degradation product of a RAFT end group containing polymer chain. The gray chemical formulas describe potential ion assignments ruled out based on higher than expected mass measurement errors. The black chemical formula describes the ion assignment confirmed via an acceptable mass measurement error. Image adapted from Figure 2 of Gruendling *et al.* [4].

ruled out based on higher than expected mass measurement errors; the mass measurement error of the third ion was reasonable, allowing a specific degradation product to be confirmed.

1.2.3 Mass Range

The mass range is the range of m/z's over which a mass analyzer can operate to record a mass spectrum. When quoting mass ranges, it is conventional to only state an upper limit; it is, however, important to note that for many mass analyzers, increasing the m/z's amenable to analysis will often compromise lower m/z measurements. As such, the mass ranges quoted for the mass analyzers described in this chapter do not necessarily reflect an absolute maximum; they instead provide an indication of the upper limits that may be achieved in standard instrumentation before performance is severely compromised.

The mass range is frequently of central importance when assessing the suitability of a given mass analyzer toward a polymer sample. For many mass analyzers, there is often a high likelihood that the polymer chains of interest are of a mass beyond the mass range; this places a severe limitation on the ability of the mass spectrometer to generate useful data. Because mass analyzers separate ions based on their m/z's, the generation of multiply charged ions may alleviate this issue. Relatively high mass resolving powers are, however, required to separate multiply charged analyte ions, and efficient and controlled multiple charging of polymer samples is generally difficult to achieve. As such, the generation of multiply charged ions is not a reliable method for overcoming mass range limitations, and for many studies, mass range capabilities will ultimately dictate a mass analyzer's suitability.

1.2.4 Linear Dynamic Range

The linear dynamic range is the range over which the ion signal is directly proportional to the analyte concentration. This measure of performance is of importance to the interpretation of mass spectral relative abundance readings; it can provide an indication of whether or not the relative abundances observed in a mass spectrum are representative of analyte concentrations within the sample. The linear dynamic range values quoted within this chapter represent the limits of mass analysis systems as integrated wholes; that is, in addition to the specific influence of the mass analyzer on linear dynamic range, the influences of ion sampling and detection have been taken into consideration. In many measurement situations, however, these linear dynamic range limits cannot be reached. Chemical- or mass-based bias effects during the ionization component of an MS experiment will frequently occur, resulting in gas-phase ion abundances that are not representative of the original analyte concentrations. When present, such ionization bias effects will generally be the dominant factor in reducing linear dynamic range. Only in the instances in which ionization bias effects can be ruled out can the linear dynamic

range values quoted in this chapter provide an indication of the trustworthiness of mass spectral abundance data.

In most polymer analyses, ionization bias effects will be prevalent. There are, however, specific scenarios in which ionization bias effects can rightfully be assumed to be minimal. One example can be found in free radical polymerizations in which propagating chains are terminated via disproportionation reactions. When considering such a system, it can be noted that disproportionation products are produced in equal abundances, but identical reaction products may also be generated from other polymerization mechanisms; accurate relative abundance data are therefore needed to infer the extent to which these other mechanisms are occurring. Because the products in question are chemically similar and have similar masses, depending on the chosen ionization method, it may be possible to conclude that these chains will not experience chemical- or mass-based ionization bias relative to each other. Under these circumstances, the linear dynamic range of the mass analysis system is crucial to the determination of accurate relative abundances for these products. This scenario can be seen in research conducted by Hart-Smith *et al.* [5], who used a 3D ion trap instrument to analyze acrylate-derived star polymers. The mass spectrum illustrated in Figure 1.4, taken from this research, shows two peaks, A and B, which correspond to disproportionation products. Based on the comparatively high relative abundance of peak B and the linear dynamic range of the 3D ion trap, these authors were able to infer that another mechanism capable of producing peak B, intermolecular chain transfer, was up to two times more prevalent than disproportionation in the polymerization under study.

1.2.5
Abundance Sensitivity

Abundance sensitivity refers to the ratio of the maximum ion current recorded at an m/z of M to the signal level arising from the background at an adjacent m/z of

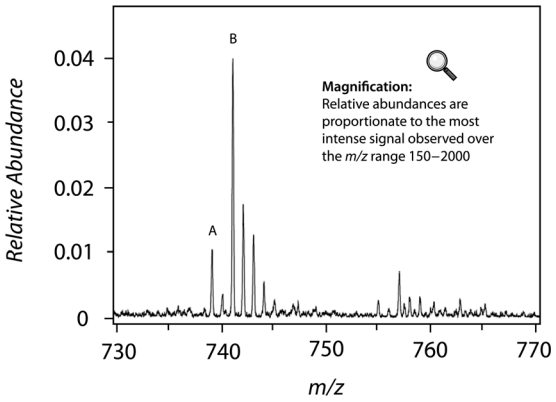

Figure 1.4 A 3D ion trap-derived mass spectrum of star polymers obtained from a RAFT-mediated polymerization of methyl acrylate, adapted from Figure 6.3.8 of Hart-Smith *et al.* [5].

($M + 1$). This is closely related to dynamic range: the ratio of the maximum useable signal to the minimum useable signal (the detection limit) [1]. Abundance sensitivity, however, goes beyond dynamic range in that it takes into account the effects of peak tailing. By considering the abundance sensitivity of a mass analyzer, one can obtain an indication of the maximum range of analyte concentrations capable of being detected in a given sample.

In the analysis of polymer samples, it is often the case that the characterization of low abundance species is of more importance than the characterization of high abundance species. For example, it is well established that polymer samples generated via RAFT polymerizations will often be dominated by chains which contain end groups derived from a RAFT mediating agent; if novel insights are to be gained into these systems, it is often required that lower abundance polymer chains are characterized. This can be seen in work conducted by Ladavière *et al.* using a time-of-flight (TOF) mass analyzer [6]. The spectrum shown in Figure 1.5, taken from this research, indicates the presence of chains with thermal initiator derived end groups (IU_x^{Na}, IY_x^{K}, and IY_x^{Na}) and chains terminated via combination reactions (C_x^{Na}), in addition to the dominant RAFT agent-derived end group containing chains. The peaks associated with termination via combination are one order of magnitude lower

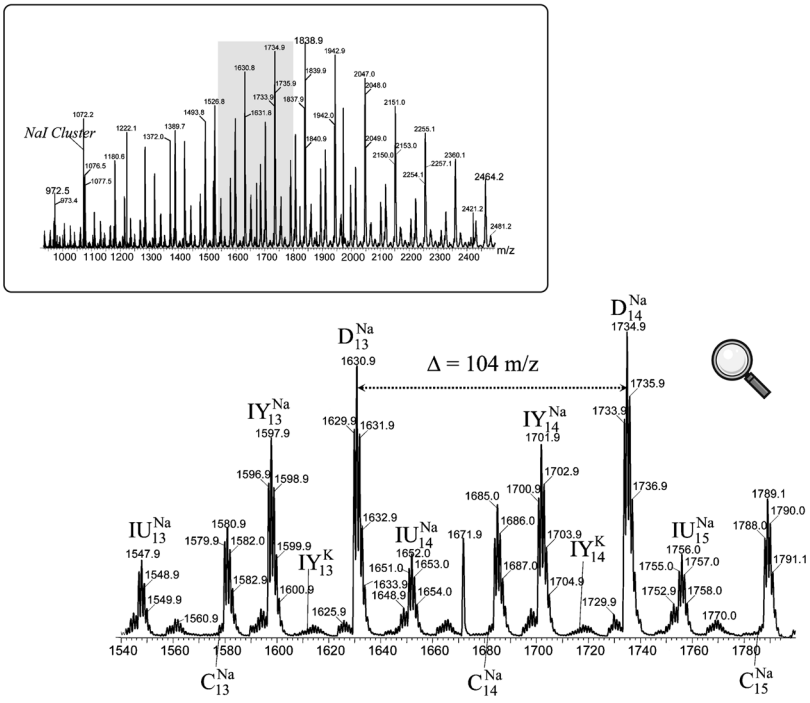

Figure 1.5 An electrospray ionization-TOF-derived mass spectrum of the polymer obtained from a RAFT-mediated polymerization of styrene, adapted from Figure 1 of Ladavière *et al.* [6].

than the most abundant peak within the spectrum and are clearly discernable from baseline noise. When attempting to characterize low abundance chains in such a manner, the abundance sensitivities listed in this chapter can provide some indication of the extent to which this can be achieved when using a given mass analyzer.

It is, however, important to note that the ability to observe relatively low abundance chains will also be influenced by components of the MS experiment other than the mass analyzer. The ionization method being used may, for example, be inefficient at ionizing the chains of interest, reducing the likelihood of their detection. The method used to prepare the polymer sample for ionization may also have an impact; for instance evidence suggests that issues associated with standard methods of polymer sample preparation for matrix-assisted laser desorption/ionization (MALDI) experiments reduce the capacity to detect relatively low abundance species [6, 7], and that these issues significantly outweigh the influence of mass analyzer abundance sensitivities [7]. The mass analyzer abundance sensitivities quoted in this chapter should therefore be contemplated alongside other aspects of MS analysis, such as those mentioned above, when designing experimental protocols for the detection of low abundance polymer chains.

1.3 Instrumentation

Since the early twentieth century, when the analytical discipline of MS was being established, many methods have been applied to the sorting of gas-phase ions according to their m/z's. The following technologies have since come to dominate mass analysis in contemporary MS and are all available from one or more commercial vendors: sector mass analyzers, quadrupole mass filters, 3D ion traps, linear ion traps, TOF mass analyzers, FT-ICR mass analyzers, and orbitraps. This section presents the basic operating principles of these instruments and summarizes their performance characteristics using the measures of performance discussed in Section 1.2. As cost and laboratory space requirements are often a determining factor in the choice of instrumentation, these characteristics are also listed.

For each mass analyzer presented in this section, the summarized performance characteristics do not necessarily represent absolute limits of performance. The use of tailored mass analysis protocols in altered commercial instrumentation, or instrumentation constructed in-house, can often allow for performance beyond what would typically be expected. The listed figures of merit, therefore, represent a summary of optimal levels of performance that should be capable of being readily accessed using standard commercially available instrumentation.

1.3.1 Sector Mass Analyzers

Sector mass analyzers are the most mature of the MS mass analysis technologies, having enjoyed widespread use from the 1950s through to the 1980s. The

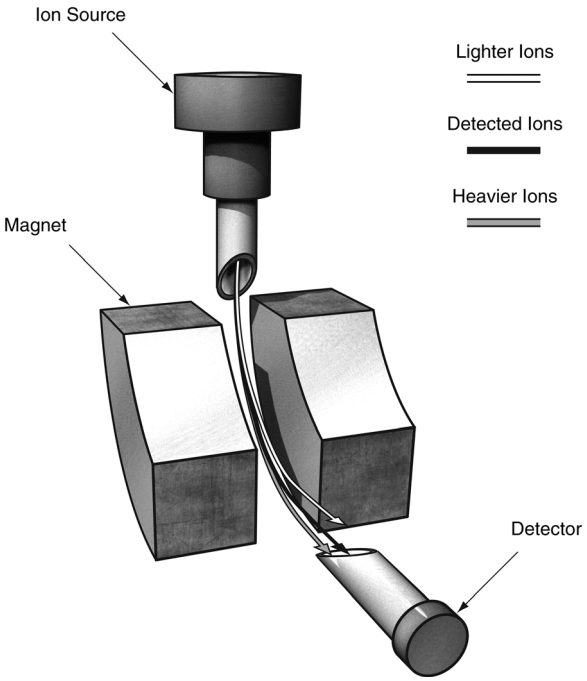

Figure 1.6 An illustration of the basic components of a magnetic sector mass analyzer system, and the means by which it achieves *m*/*z*-based ion separation.

illustration in Figure 1.6 demonstrates the basic operating principle of magnetic sectors, which are employed in all sector mass analyzers. Magnetic sectors bend the trajectories of ions accelerated from an ion source into circular paths; for a fixed accelerating potential, typically set between 2 and 10 kV, the radii of these paths are determined by the momentum-to-charge ratios of the ions. In such a manner, the ions of differing *m*/z's are dispersed in space. While dispersing ions of different momentum-to-charge ratios, the ions of identical momentum-to-charge ratios but initially divergent ion paths are focused in a process called direction focusing. These processes ensure that, for a fixed magnetic field strength, the ions of a specific momentum-to-charge ratio will follow a path through to the ion detector. By scanning the magnetic field strength, the ions of different *m*/*z* can therefore be separated for detection.

When utilizing a magnetic sector alone, resolutions of only a few hundred can be obtained. This is primarily due to limitations associated with differences in ion velocities. To correct for this, electric sectors can be placed before or after the magnetic sector in "double focusing" instruments, as illustrated in Figure 1.7. Electric sectors disperse ions according to their kinetic energy-to-charge ratios, while also providing the same type of direction focusing as magnetic sectors. Through the careful design of two sector instruments, these kinetic energy dispersions can be corrected for by the momentum dispersions of the magnetic

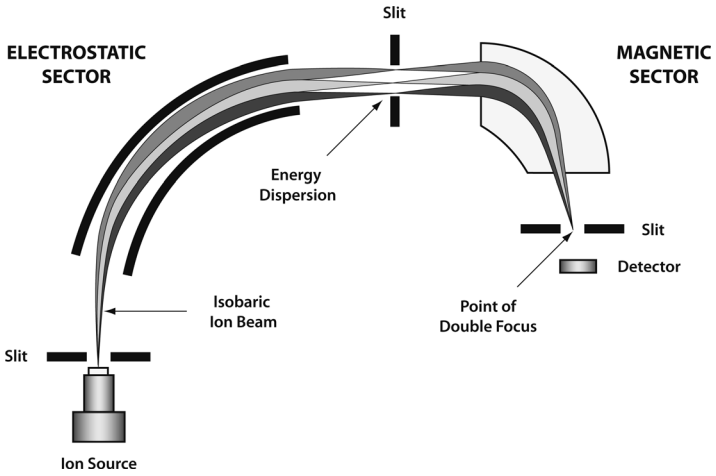

Figure 1.7 The operating principles of a double focusing sector mass analyzer.

sector. This results in velocity focusing, where ions of initially differing velocities are focused onto the same point. As both sectors also provide direction focusing, differences in both ion velocities and direction are accounted for in this process of double focusing.

The performance characteristics of double focusing sector instruments, as listed in Table 1.1, are unrivaled in terms of linear dynamic range and abundance sensitivity, while excellent mass accuracy and resolution are also capable of being obtained [8]. Despite these high-level performance capabilities, which have largely been established in elemental and inorganic MS, the use of sector mass analyzers in relation to other instruments has declined. This is because the applications of MS to biological problems, which have driven many of the contemporary advances in mass analyzer design, do not place an emphasis on obtaining ultrahigh linear dynamic ranges or abundance sensitivities. When coupled with the prohibitive size and cost of sector mass analyzers, this has seen other mass analyzer technologies favored by commercial producers of MS instrumentation. As such, sector mass analyzers have not been widely implemented in the analysis of macromolecules, such as synthetic polymers.

Table 1.1 Typical figures of merit for double focusing sector mass analyzers.

Mass resolving power	100 000
Mass accuracy	<1 ppm
Mass range	10 000
Linear dynamic range	1×10^9
Abundance sensitivity	1×10^6–1×10^9
Other	High cost and large space requirements

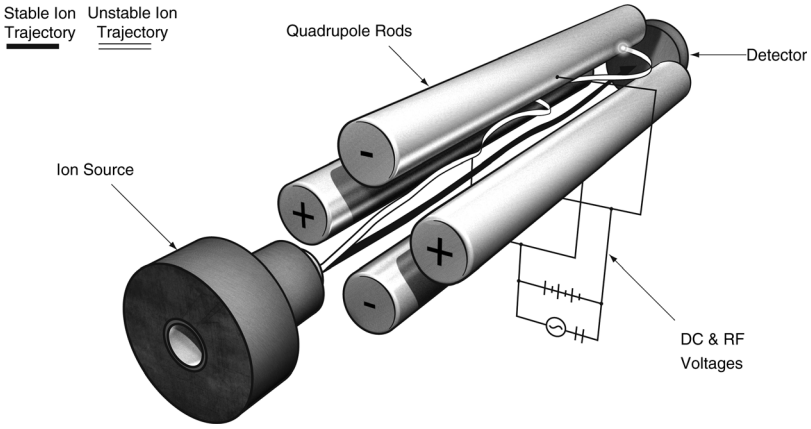

Figure 1.8 An illustration of the basic components of a quadrupole mass filter system, and the means by which it achieves *m/z*-based ion separation.

1.3.2 Quadrupole Mass Filters

Since the 1970s quadrupole mass filters have been perhaps the most widely utilized mass analyzer. The basic features of this method of mass analysis are illustrated in Figure 1.8. Quadrupole mass filters operate via the application of radio frequency (RF) and direct current (DC) voltages to four rods: the combination of RF and DC voltages determine the trajectories of ions of a given *m/z* within the mass filter; stable ion trajectories pass through to the detector while ions of unstable trajectories are neutralized by striking the quadrupole electrodes. By increasing the magnitude of the RF and DC voltages, typically while keeping the ratio of these two different voltages constant, the ions of differing *m/z* can sequentially pass through the mass filter for detection.

In discussing the operation of quadrupole mass filters, Mathieu stability diagrams are often of great utility. These diagrams, an example of which has been shown in Figure 1.9, allow one to obtain a ready visualization of the ions which will pass through to the detector and the ions which will not. The equations of ion motion in a quadrupole mass filter are second-order differential equations – this is because the RF voltages applied during mass analysis are time varying – and Mathieu stability diagrams are graphical representations of general solutions to these second-order differential equations. They are produced by plotting a parameter related to the RF voltage, *q*, against a parameter related to the DC voltage, *a*. These parameters are also determined by the frequency of the RF voltage, the size of the quadrupole rods and the *m/z*'s of the ions under scrutiny. As the size of the quadrupole rods remain unchanged and the frequency of the RF voltage is usually held constant, one can therefore readily observe voltage combinations that will lead to stable trajectories for ions of a specified *m/z*. These areas in the Mathieu stability diagram are termed stability regions, and are labeled A, B, C, and D in Figure 1.9.

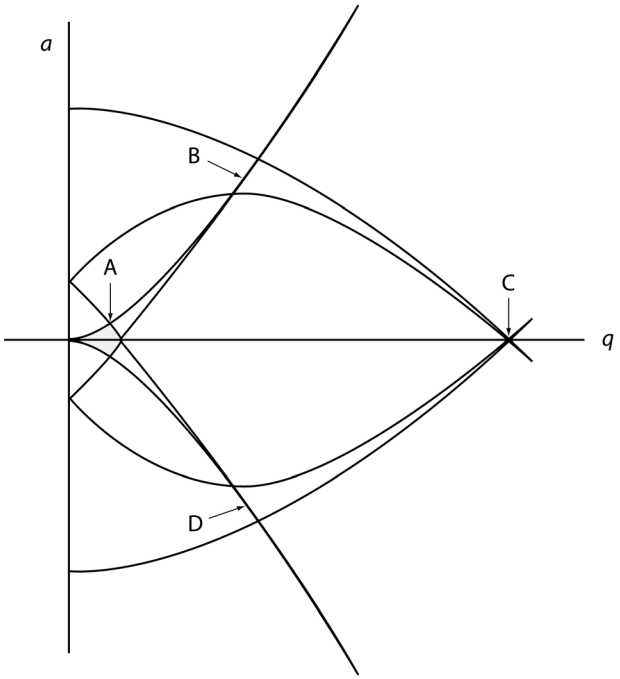

Figure 1.9 The Mathieu stability diagram. Stability regions are labeled A, B, C, and D.

Typical figures of merit for quadrupole mass filters have been listed in Table 1.2. Though quadrupole mass filters are a mainstay of contemporary mass analysis, they are low-performance instruments when judged in terms of mass resolving power, mass accuracy, and mass range. The vast majority of quadrupole mass filters operate within the first stability region, labeled A in Figure 1.9, and improvements in mass resolving power have been demonstrated when operating in higher stability regions [9, 10]. These improvements, however, come at the expense of mass range. Likewise, mass range extensions, which have been achieved through reductions in the operating frequency of the RF voltage [11–14], come at the expense of mass resolving power. The inability to maximize mass range, mass resolving power, or mass accuracy without compromise has ensured that, when operating quadrupole mass filters under standard conditions, these performance characteristics remain

Table 1.2 Typical figures of merit for quadrupole mass filters.

Mass resolving power	100–1000
Mass accuracy	100 ppm
Mass range	4000
Linear dynamic range	1×10^7
Abundance sensitivity	1×10^4–1×10^6
Other	Low cost and low space requirements

modest. Despite these limitations, quadrupole mass filters are capable of producing excellent linear dynamic ranges and abundance sensitivities. Along with their low cost, ease of automation, low ion acceleration voltages, and small physical size, these performance capabilities have contributed to the continued popularity of these instruments.

1.3.3 3D Ion Traps

Quadrupole ion traps are close relatives of the quadrupole mass filter and may be employed as 2D or 3D devices. The present section focuses upon the 3D ion trap, an example of which has been illustrated in Figure 1.10. The operating principles of 3D ion traps are similar to those of quadrupole mass filters. 3D ion traps, however, apply their electric fields in three dimensions as opposed to the two dimensions of mass filters; this is achieved through the arrangement of electrodes in a sandwich geometry: two end-cap electrodes enclose a ring electrode. This arrangement allows ions to be trapped within the electric field. When considering the operating principles of 3D ion traps, the Mathieu stability diagram may once again be used to visualize the

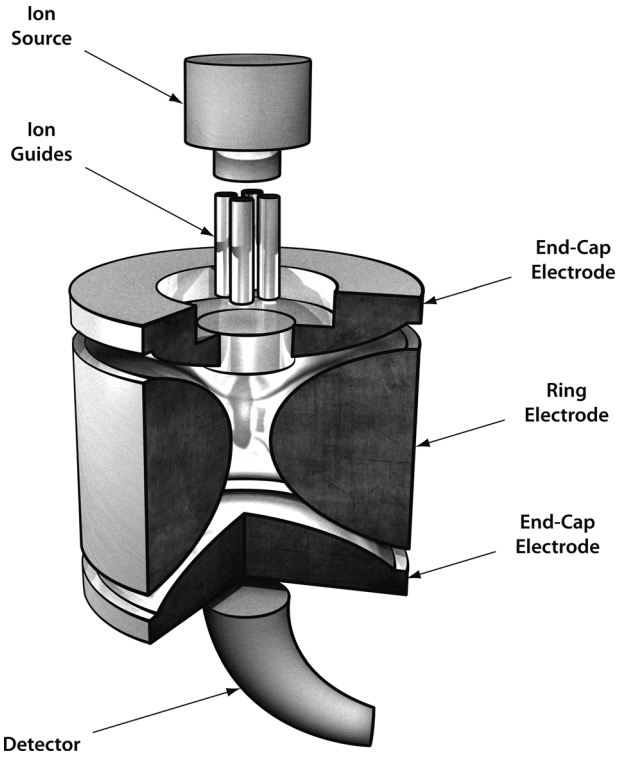

Figure 1.10 An illustration of the basic components of a 3D ion trap system.

Table 1.3 Typical figures of merit for 3D ion traps.

Mass resolving power	1000–10 000
Mass accuracy	50–100 ppm
Mass range	4000
Linear dynamic range	1×10^2–1×10^3
Abundance sensitivity	$1 \times 10^2 - 1 \times 10^3$
Other	Low cost and low space requirements

ions selected for detection. Unlike quadrupole mass filters, however, it is the unstable ions that are detected in standard 3D ion trap mass analysis. Mass selective instability is introduced by scanning the RF voltage applied to the device; as the voltage increases, the ions of sequentially higher m/z's are selected for detection by being ejected through an end-cap opening.

3D ion traps are generally capable of achieving moderate levels of performance in terms of mass resolving power, mass accuracy, and mass range, as can be seen in the figures of merit listed in Table 1.3. Innovative modes of operation can, however, allow these performance characteristics to be improved. For example, mass range extensions can be achieved by using resonance ejection, in which resonance conditions are induced by matching the frequency of ion oscillations in the trap with the frequency of a supplementary potential applied to the end-cap electrodes. Large enough amplitude of the resonance signal will allow ions to be ejected from the trap. Mass ranges of approximately 70 000 have been observed in conventional 3D ion traps using resonance ejection [15, 16], though this mode of operation is not readily supported by commercial instrumentation. The substantial lowering of RF voltage scan rates is another method by which 3D ion trap performance can be improved. Using this technique, resolutions of up to 10^7 have been achieved [17]. Such high levels of performance, however, come at the expense of analysis time and are generally performed over narrow mass ranges. As such, practical operating conditions result in significantly lower mass resolving powers.

The linear dynamic ranges of ion trapping devices, such as 3D ion traps, are limited by mass discrimination effects associated with ion/ion interactions or charge transfer to background gases. The extents to which these effects occur are influenced by ion trap storage capacities. In 3D ion traps, mass discrimination effects can ultimately lead to quite low performance. Though methods based around the selective accumulation of specific ions have been shown to increase linear dynamic range up to at least 10^5 [18], these methods rely upon preselection of ions for analysis and are therefore unlikely to be practical for most polymer studies.

The abundance sensitivities of 3D ion traps are also relatively low. As with the linear dynamic range, the abundance sensitivity is related to the ion storage capacity when an ion trapping device is employed. The ion storage capacity of a specific device will depend on its dimensions and operating parameters, but in general, commercial 3D ion traps can be estimated to be capable of trapping 10^6–10^7 ions [19]. Though attempts at increasing abundance sensitivity have been made [20, 21], the inherent

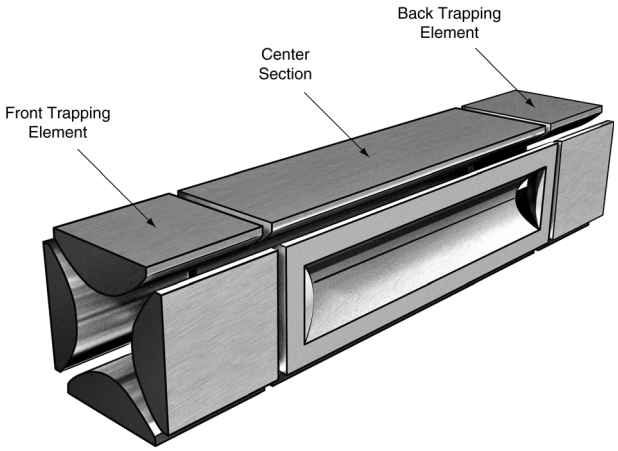

Figure 1.11 An illustration of the basic components of a radial ejection linear ion trap.

limitations of 3D ion trap storage capacity ensure that the abundance sensitivities of these instruments remain a weakness.

Despite their relatively modest performance capabilities, commercial ion traps are highly robust, have impressive MS/MS and MS^n capabilities (as expanded upon in Section 1.4) and are also remarkable for their attractively low size and cost. As such, 3D ion traps continue to see widespread use as workhorse-type instruments.

1.3.4
Linear Ion Traps

The operation of a quadrupole ion trap as 2D device – a linear ion trap – was first described in the late 1960s, but it is only in recent years that linear ion traps have emerged as a prominent form of mass analyzer. In contemporary stand-alone linear ion traps [22], an example of which has been illustrated in Figure 1.11, ions are trapped radially in a central section by an RF voltage, and axially by static DC potentials applied to end trapping elements. As with 3D ion traps, ions associated with unstable regions in the Mathieu stability diagram are selected for detection. The mass selective ejection of ions occurs radially through slots in central section rods and is achieved via the application of alternating current (AC) voltages. In addition to these stand-alone radial ejection devices, axial ejection linear ion traps have also found utility in contemporary MS by enhancing the performance of triple quadrupole (QqQ) mass spectrometers [23]; the basic capabilities of QqQ instruments will be discussed in Section 1.4.

Typical figures of merit for linear ion traps have been listed in Table 1.4. The mass resolving powers, mass accuracies, and mass ranges of linear ion traps are controlled by many of the processes associated with 3D ion trap mass analysis; as such, the capabilities of these two forms of mass analyzer are comparable when using these measures of performance. Linear ion traps do, however, feature ion storage capacities

Table 1.4 Typical figures of merit for linear ion traps.

Mass resolving power	1000–10 000
Mass accuracy	50–100 ppm
Mass range	4000
Linear dynamic range	1×10^3–1×10^4
Abundance sensitivity	1×10^3–1×10^4
Other	Low cost and low space requirements

that are over an order of magnitude higher than those of 3D ion traps [24]; the associated decreases in mass discrimination [22] suggest that greater linear dynamic range capabilities should be expected from these instruments. The trapping efficiencies of linear ion traps have also been demonstrated to be superior to those of 3D ion traps [22]. This advantage, in concert with their superior ion storage capacities, leads to relatively high abundance sensitivities. Like 3D ion traps, linear ion traps also feature high levels of robustness, excellent MS/MS and MS^n capabilities, favorably small size, and relatively low costs. When coupled to their superior performance capabilities, these features suggest that linear ion traps will likely supplant 3D ion traps as the dominant technology in quadrupole ion trap mass analysis.

1.3.5 Time-of-Flight Mass Analyzers

The 1980s witnessed the development of the revolutionary pulsed ionization method of MALDI. The mass analysis technique that saw the greatest increase in prominence as a result of this development was the TOF process, which requires a well-defined start time and is therefore ideally suited to being interfaced with pulsed ion sources. Though various important advances have been made to the TOF process since the development of MALDI, the basic operating principles underlying this method of mass analysis remain conceptually simple. These basic principles of operation can be seen in the illustration shown in Figure 1.12. All TOF mass analyzers rely upon the acceleration of ions obtained from an ion source through a fixed potential into a drift region of a set length. This process of ion acceleration results in all ions of the same charge obtaining the same kinetic energy, and as kinetic energy is equal to $0.5\ mv^2$, with m representing the mass of the ion and v the velocity of the ion, lower mass ions will obtain a greater velocity than higher mass ions. Lower mass ions will therefore traverse the distance of the drift region in a shorter amount of time than heavier ions, resulting in the separation of ions according to their m/z. As the length of the drift region is known, ion velocities can be determined by measuring the time they take to reach the detector, allowing the m/z of the ions to be determined.

An important source of error in a TOF experiment stems from small differences in the kinetic energies of ions of the same m/z; when MALDI ion sources are used, these kinetic energy distributions can be traced to aspects inherent to the complex processes involved in gas-phase ion generation [25]. To correct for these differences, almost all

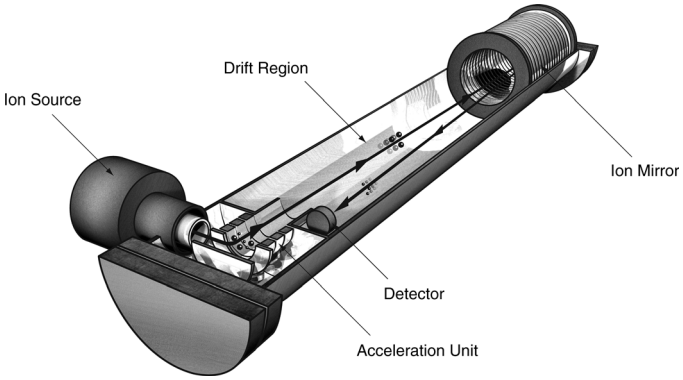

Figure 1.12 An illustration of the basic components of an orthogonal acceleration TOF mass analysis system featuring an ion mirror, and the means by which it achieves *m/z*-based ion separation.

TOF mass analyzers employ a single ion mirror, as illustrated in Figure 1.12. These reflectron TOF instruments operate by sending ions down one flight distance toward an electrostatic mirror, which then reflects the ions down a second flight distance toward a detector. In addition to compensating for differences in ion kinetic energies, the use of an ion mirror has the additional advantage of increasing the total flight distance without having to significantly increase the size of the mass spectrometer. These improvements lead to significantly increased mass resolving power and mass accuracy [26]. Kinetic energy distributions can also be corrected for through the process of delayed extraction, in which MALDI is performed in the absence of an electric field; ions are subsequently extracted using a high voltage pulse after a predetermined time delay. This process of delayed extraction has also been demonstrated to produce significant improvements in mass resolving power and mass accuracy [27–29].

Another major advance in contemporary TOF mass analysis has been the invention of orthogonal acceleration for coupling to continuous ionization sources [30], the basic principles of which are also illustrated in Figure 1.12. This technique makes use of independent axes for ion generation and mass analysis; a continuous ion source fills an acceleration region, and when full, an orthogonal acceleration process sends the ions into the TOF drift region. While the ions are being separated in the drift region, a new set of ions is collected in the acceleration region; this produces great experimental sensitivity. Importantly, orthogonal acceleration TOF has allowed ionization methods other than MALDI, most notably electrospray ionization (ESI), to benefit from the strong performance characteristics of TOF mass analysis.

Typical figures of merit for TOF mass analyzers are given in Table 1.5. Most contemporary TOF mass analyzers are reflectron instruments; the quoted mass resolving power and mass accuracy values are based upon the capabilities of these mass spectrometers. The mass accuracy values obtained from contemporary instrumentation have also benefited from the development of increasingly fast electronics; the nanosecond time resolution that is now routinely available contributes to the potential for achieving excellent mass accuracy. Increasingly fast electronics have also

Table 1.5 Typical figures of merit for TOF mass analyzers.

Mass resolving power	1000–40 000
Mass accuracy	5–50 ppm
Mass range	>100 000
Linear dynamic range	1×10^6
Abundance sensitivity	1×10^6
Other	Moderate cost and moderate space requirements

contributed toward increases in linear dynamic range. As there is a trade-off between the speed of the electronics and dynamic range, the capabilities of digital electronics improve the point at which this trade-off occurs. In terms of abundance sensitivity, the phenomenon of detector ringing as a result of higher abundance ion detection can have an adverse impact [31]. This problem is, however, minor when compared to the issues related to ion storage capacities in ion trapping instruments; TOF mass analyzers therefore typically feature higher levels of abundance sensitivity when compared to ion trapping devices. Of particular importance to polymer chemists is the mass range of TOF mass analyzers, which is theoretically unlimited. Mass ranges of 2000 kDa have been demonstrated in a cryodetection MALDI-TOF instrument [32], and in practice, mass ranges of >70 000 can be readily achieved using commercial instrumentation. In combination, these performance characteristics make TOF mass analysis an incredibly attractive option for many polymer studies.

1.3.6
Fourier Transform Ion Cyclotron Resonance Mass Analyzers

Mass analysis by FT-ICR was first described in 1974 [33], and the method has since grown to become the state of the art in terms of mass resolving power and mass accuracy capabilities. The basic operating principles of FT-ICR mass analysis are illustrated in Figure 1.13. In a similar manner to magnetic sector-based mass analysis, FT-ICR utilizes a magnetic field in its determinations of m/z. The kinetic energies of the ions measured by FT-ICR are, however, significantly lower than those analyzed by magnetic sector mass analyzers; this has the important consequence that, rather than being deflected by the magnetic field, the ions are trapped within the magnetic field. These trapped ions orbit with "cyclotron" frequencies that are inversely proportional to their m/z. Following the trapping of ions, RF voltages on excitation plates held perpendicular to the magnetic field are swept through a range of frequencies; this causes the sequential resonance excitation of ions into higher radii orbits. The oscillating field generated by these ion ensembles induces image currents in circuits connected to detection plates; the resultant time-domain signals of ion motion are converted into frequency-domain signals via a Fourier transform, which leads to the generation of a mass spectrum. If low pressures are maintained within the FT-ICR cell, the cyclotron motion can be held for many cycles, reducing the uncertainty of the frequency measurements and thereby allowing m/z to be determined with great accuracy.

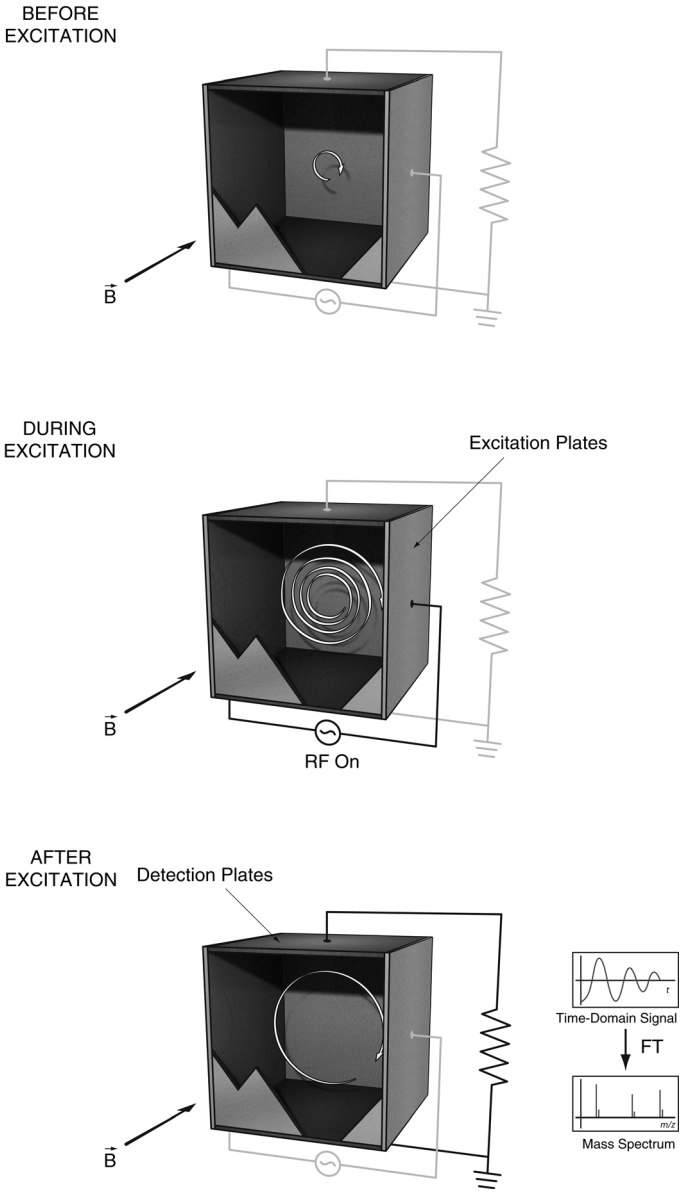

Figure 1.13 The operating principles of FT-ICR mass analysis. White arrows represent illustrative ion paths.

A summary of typical figures of merit for FT-ICR mass analyzers is given in Table 1.6. The mass resolving power and mass accuracy capabilities of these instruments are unparalleled in contemporary MS, and significant opportunities exist for these capabilities to be improved even further [34]. FT-ICR instruments also

Table 1.6 Typical figures of merit for FT-ICR mass analyzers.

Mass resolving power	10 000–1000,000
Mass accuracy	1–5 ppm
Mass range	>10 000
Linear dynamic range	1×10^3–1×10^4
Abundance sensitivity	1×10^3–1×10^4
Other	High cost and large space requirements

offer increased mass ranges relative to other ion trapping devices. Ion storage capacities, however, remain to be a determining factor in limiting linear dynamic ranges and abundance sensitivities. Despite this, FT-ICR mass analyzers are the highest quality option for the analysis of polymer samples when ultrahigh mass accuracy and resolving power are required. These advantages do, however, come at a premium in terms of instrument cost and laboratory space requirements.

1.3.7 Orbitraps

Orbitraps represent the most recently developed form of mass analyzer in widespread contemporary usage, having been first described in 2000 [35]. The general principles of operation associated with orbitrap mass analysis are illustrated in Figure 1.14. These mass analyzers, like FT-ICR instruments and quadrupole ion traps, function as ion trapping devices. Unlike these other mass analyzers, however, orbitraps perform their trapping functions in the absence of magnetic or RF fields and instead utilize a purely electrostatic field generated by an outer barrel-like electrode and an inner axial spindle. Ions are injected tangentially into this field. The electrodes are carefully shaped such that the electrostatic attractions of the ions to

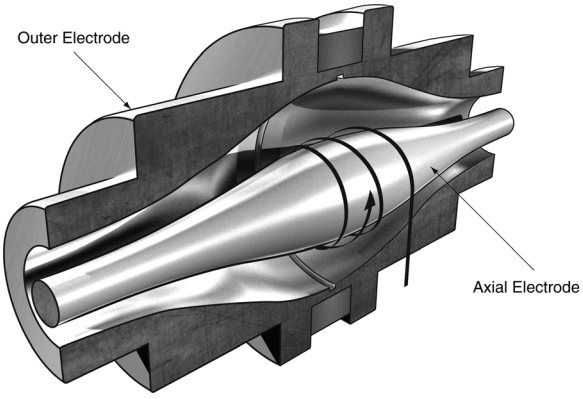

Figure 1.14 An illustration of the basic components of an Orbitrap mass analyzer. The black arrow represents an illustrative ion path.

Table 1.7 Typical figures of merit for orbitrap mass analyzers.

Mass resolving power	10 000–150 000
Mass accuracy	2–5 ppm
Mass range	6000
Linear dynamic range	1×10^3–1×10^4
Abundance sensitivity	1×10^4
Other	Moderate cost and low space requirements

the inner electrode are balanced by their centrifugal forces, causing them to orbit around the spindle, while the axial field causes the ions to simultaneously perform harmonic oscillations along the spindle at a frequency proportional to $(m/z)^{0.5}$. Image currents induced by the oscillating ions are detected by the outer wall of the barrel-like chamber, and in a similar manner to FT-ICR, the resultant time-domain signals of ion motion are converted into frequency-domain signals via a Fourier transform, which allows a mass spectrum to be produced.

A summary of typical figures of merit associated with orbitrap mass analyzers is presented in Table 1.7. As with FT-ICR, the mass resolving powers obtained using orbitraps are proportional to the number of harmonic oscillations that are detected. As the maximum acquisition times in orbitraps are more limited than those of FT-ICR instruments, their mass resolving power ceilings are not as high. Nevertheless, orbitraps are still capable of achieving mass resolving powers of up to 150 000 [36], which places them among the most powerful instruments available today. The mass accuracy values capable of being obtained using orbitraps approach those of FT-ICR instruments; mass accuracies within 2 ppm can be expected when internal calibration is performed [37]. Though issues relating to ion storage capacity still place significant limitations on the capabilities of orbitraps in relation to linear dynamic range and abundance sensitivity, they nonetheless feature larger ion storage capacities [35–38] and greater space charge capacities at higher mass [39] when compared to FT-ICR mass analyzers and 3D ion traps. As such, orbitraps have been shown to compare favorably with these instruments when judged by these particular measures of performance [36]. A major advantage of orbitraps is that their functioning does not require the use of superconducting magnets; they are therefore significantly less costly than FT-ICR instruments and have far more modest laboratory space requirements. These factors may ultimately ensure that orbitraps become favored over FT-ICR instruments for ultrahigh mass resolving power and mass accuracy polymer in analyses.

1.4 Instrumentation in Tandem and Multiple-Stage Mass Spectrometry

Developments in ion source, mass analyzer, and detector technologies have significantly improved the performance characteristics of modern mass spectrometers (*vide supra*). While these improvements have contributed greatly to the utility of MS in

polymer science by more sensitive and accurate measurement of m/z, understanding the structural connectivity of molecular species cannot be established by molecular mass alone no matter how accurately measured. In other disciplines, MS/MS as well as MS^n have greatly expanded the scope and utility of MS by providing structural elucidation. Nowhere is this more apparent than in proteomics where the sequences (i.e., molecular structure) of peptide biopolymers are now established, almost exclusively, by this approach. Comparatively, the implementation of MS/MS and MS^n in polymer characterization has been modest and this can be attributed to two key reasons: (i) the yield of product ions observed is often low and (ii) the greater heterogeneity in synthetic polymer samples makes interpretation of the data challenging [40, 41]. While MS/MS and MS^n of polymers is the topic of a further chapter of this book, here we discuss the key performance criteria of different combinations of mass analyzers and highlight some contemporary developments that may play a role in overcoming some of the current challenges in generating information-rich tandem mass spectra of polymers.

MS/MS involves two stages of MS: precursor ions are mass-selected in the first stage (MS-I) of the experiment and are induced to undergo a chemical reaction that changes their mass or charge, leaving behind a product ion and a neutral fragment (or possibly another product ion if the precursor ion was multiply charged); in the second stage (MS-II), the product ions generated from these chemical reactions are mass analyzed. Some instruments allow this process to be repeated multiple times in MS^n experiments, where n refers to the number of stages of MS performed. The chemical reactions that proceed between the different MS stages are most frequently unimolecular dissociation reactions initiated by an increase in internal energy. Such ion activation is most commonly affected by collision-induced dissociation (CID), whereby the mass-selected precursor ion undergoes an energetic collision with an inert, stationary gas (e.g., N_2, Ar, or He) [42]. The amount of energy imparted in the collision is related to the translational kinetic energy of the precursor ion (most easily considered as the product of the number of charges on the ionized molecule and the accelerating potential applied within the instrument) and its mass. Thus, for ionized oligomers if the mass increases without a concomitant increase in charge, the internal energy will be less resulting in a lower product ion abundance.

Various different scan types can be executed in MS/MS and MS^n experiments, and each type can be used to extract different pieces of information from the sample under investigation. These scan types, as summarized in Figure 1.15 for MS/MS experiments, depend upon the static (i.e., transmission of a single m/z) or scan (i.e., analysis of all m/z) status of each stage of the experiment. How these different scan types apply to investigations concerning polymer systems are expanded upon below.

Selected reaction monitoring is generally implemented for the purposes of selective ion quantification and involves passing a known precursor ion through MS-I, and a known product ion (or ions) through MS-II. In this manner, precursor ions of indistinguishable mass to other ions generated from the sample can be selectively monitored if they produce unique product ions. Added specificity can be obtained by undertaking multiple-reaction monitoring experiments where, for example, several product ions are monitored in MS-II. Such analyses are usually

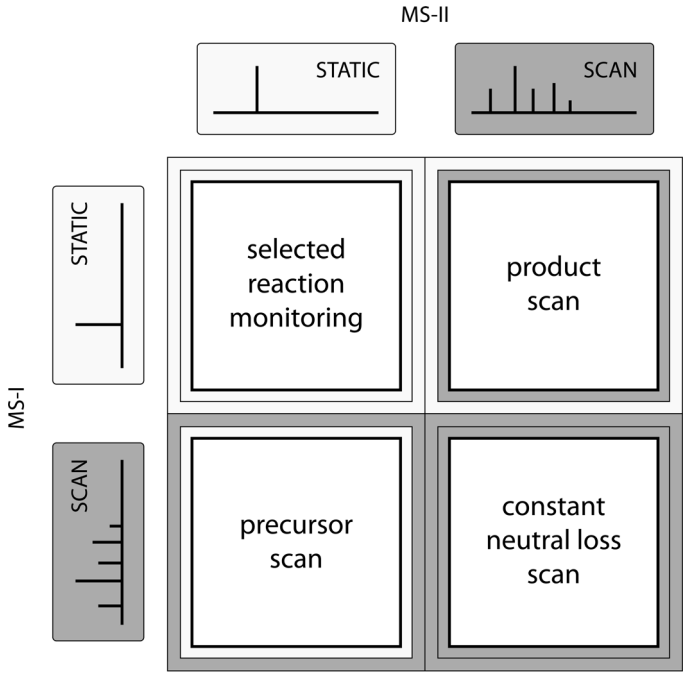

Figure 1.15 A summary of the scan types available to MS/MS experiments.

performed as a mechanism for highly selective and sensitive detection in online liquid or gas chromatography (i.e., LC-MS/MS and GC-MS/MS). Though these experiments can be of enormous utility for various purposes, for example, in the quantification of pharmaceutical compounds in human plasma, selected reaction monitoring has limited value in the majority of conventional MS investigations into polymerization systems. This lies in the fact that polymerization experiments typically couple poorly to conventional chromatographic methods and often fragmentation of the systems in question has not previously been established.

As with selected reaction monitoring, the precursor ion scan type requires knowledge of the preferred modes of fragmentation for the precursor ions. This particular scan type allows for the selective detection of particular classes of precursor ions, namely, precursor ions which dissociate to form common product ions. The precursor scan type can be of use in the analysis of polymer samples if the fragmentation behavior for a given ion obtained from the sample is known. Using this information, other structurally similar ions can be identified, potentially simplifying the identification of products in the sample. In a similar way, the constant neutral loss scan monitors a neutral mass loss between precursor and product ion and thus can also be used for monitoring for molecules with a similar structural motif in the presence of other, more abundant but structurally unrelated compounds. In a neutral loss scan, MS-I and MS-II are scanned to maintain a constant m/z difference associated with the neutral fragment of interest. In a similar manner to the precursor

scan, the constant neutral loss scan can be used to identify ions of a common structural background, which can potentially aid in product identification. While this combination of scan types has been used to great effect in other fields, notably lipid MS [43], it has yet to be widely applied in polymer characterization because of the wide range of polymer structures and only a limited knowledge of fragmentation behavior.

Of the four scan types in MS/MS, the product ion scan is the most direct method of obtaining structural information from a previously unidentified ion and is thus perhaps the most widely applicable to samples associated with investigations into polymer systems. The product scan type isolates a specific precursor ion and analyzes all of the resulting product ions; careful interpretation of the fragmentation pathways indicated by the product ions can allow insights into the structural make-up of the precursor ion.

The instruments capable of undertaking MS/MS experiments can be classified into two groups: tandem-in-space instruments and tandem-in-time instruments. Tandem-in-space instruments require separate mass analyzers to be utilized for each MS stage and are associated with beam-type technology such as sector mass analyzers, quadrupole mass filters, and TOF mass analyzers. The earliest MS/MS instruments used sectors for the two MS stages [44], and the promise shown by these instruments led to the development of the cheaper and more user-friendly QqQ [45]. These QqQ instruments, which are still heavily in use today, operate the first and last quadrupoles as the actual mass filters, with the middle quadrupole acting as a CID cell. Since the introduction of QqQ instruments, various hybrid instruments, in which distinct mass analysis methodologies are applied at each stage of the MS/MS experiment, have been developed. Of these instruments, the quadrupole-TOF (Q-TOF) mass spectrometer [46] has become a mainstay of MS/MS technology. Q-TOF instruments have the disadvantage of not being able to perform the precursor and constant neutral loss scans that QqQ instruments are capable of, as the TOF method of separating ions in time is not conducive to these screening-type scans; however, these instruments remain advantageous for the speed in which MS/MS experiments can be conducted and their ability to provide accurate mass measurements on product ions. In contrast to the tandem-in-space instruments, tandem-in-time instruments separate the different MS stages by time, with the various stages of MS/MS being performed in one mass analyzer. These instruments are associated with ion trapping technology such as quadrupole ion traps, FT-ICR mass analyzers, and orbitraps. Though tandem-in-time instruments are incapable of performing precursor ion or constant neutral loss scans, they have the advantage of being able to readily perform MS^n experiments, as the separate MS stages do not require the implementation of multiple mass analyzers. This can be advantageous in providing detailed structural information by elucidation of secondary or even tertiary product ions. More recently, hybrid instruments have been developed that combine both in-space with in-time mass analysis leading to a fascinating array of combinations, as summarized in Figure 1.16.

While a detailed discussion of the relative capabilities of the instrument geometries listed in Figure 1.16 is beyond the scope of this chapter (see Ref. [47]), one key criterion that should be considered in the context of MS/MS is the collision energy

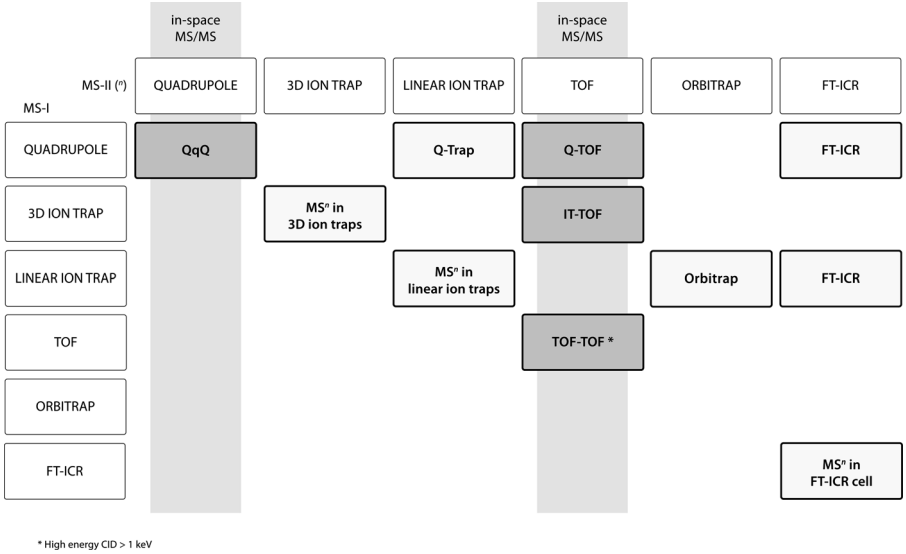

Figure 1.16 A summary of mass analyzers and mass analyzer combinations used for MS/MS and MS^n.

regime (an excellent tutorial on the full range of figures of merit in ion activation is found in Ref. [48]). Depending on the instrument configuration, CID is generally considered as either high or low energy depending on whether the translational energy of the precursor ion is $>$ or $<$1 keV, respectively. Early sector-based mass spectrometers operated in the keV energy range, and thus the mechanism of ion activation and the amount of internal energy imparted to a precursor ion was significantly different to that of a contemporary QqQ or Q-TOF geometry instrument (typically $<$100 eV). Interestingly, more recent developments in TOF-TOF geometries have, almost serendipitously, provided renewed interest in the high-energy CID regime. This holds out some promise for polymer analysis where oligomers can be of high mass and may be only singly charged [49]. Furthermore, the current research into alternative approaches to ion activation and their implementation into commercial instrumentation (e.g., electron capture dissociation, electron transfer dissociation, and photodissociation) augurs well for future development of tandem mass spectrometric methods for polymer science.

1.5 Conclusions and Outlook

Recent and continuing advances in mass analyzer design have ensured that the field of polymer chemistry remains well positioned to see increased benefits from MS. Workhorse-type instruments, such as quadrupole ion traps, are now well established, and their role in providing readily accessible, informative polymer characterizations

is unlikely to be displaced in the near future. With the growing accessibility of high performance mass analysis options, a general increase in the depth of mass spectrometric-based polymer characterizations can, however, be envisaged. In this regard, the benefits of ultra high mass accuracy and mass resolving power, previously obtained solely from FT-ICRs for polymer samples, are likely to become more broadly appreciated with the advent of orbitrap mass analysis. The increasing power of TOF technologies is also of note; progressively higher mass accuracies and resolving powers are being achieved over broad mass ranges. Along with their potential to produce excellent abundance sensitivities, these improving performance characteristics suggest that TOF mass analyzers will continue to play an important role in polymer chemistry. Though continued progress in individual mass analyzer design can be expected, the dominant trend in contemporary MS instrument development has been in mass analyzer hybridization. The specific benefits of these hybrid instruments will become more apparent as the role of MS/MS and MS^n in polymer chemistry is further established. Given this suite of new and developing technologies, an intriguing array of mass analysis options is now primed to be more thoroughly explored by the polymer chemistry community.

References

1 McNaught, A.D. and Wilkinson, A. (1997) BT IUPAC Compendium of Chemical Terminology, Blackwell Scientific Publications, Oxford.

2 Szablan, Z., Junkers, T., Koo, S.P.S., Lovestead, T.M., Davis, T.P., Stenzel, M.H., and Barner-Kowollik, C. (2007) Mapping photolysis product radical reactivities via soft ionization mass spectrometry in acrylate, methacrylate, and itaconate systems. *Macromolecules*, **40** (19), 6820–6833.

3 Brenton, A.G. and Godfrey, A.R. (2010) Accurate mass measurement: Terminology and treatment of data. *J. Am. Soc. Mass Spectrom.*, **21** (11), 1821–1835.

4 Gruendling, T., Pickford, R., Guilhaus, M., and Barner-Kowollik, C. (2008) Degradation of RAFT polymers in a cyclic ether studied via high resolution ESI-MS: Implications for synthesis, storage, and end-group modification. *J. Polym. Sci. Pol. Chem.*, **46** (22), 7447–7461.

5 Hart-Smith, G., Chaffey-Millar, H., and Barner-Kowollik, C. (2008) Living star polymer formation: detailed assessment of poly(acrylate) radical reaction pathways via ESI-MS. *Macromolecules*, **41** (9), 3023–3041.

6 Ladavière, C., Lacroix-Desmazes, P., and Delolme, F. (2009) First systematic MALDI/ESI mass spectrometry comparison to characterize polystyrene synthesized by different controlled radical polymerizations. *Macromolecules*, **42** (1), 70–84.

7 Hart-Smith, G., Lammens, M., Du Prez, F.E., Guilhaus, M., and Barner-Kowollik, C. (2009) ATRP poly(acrylate) star formation: A comparative study between MALDI and ESI mass spectrometry. *Polymer*, **50** (9), 1986–2000.

8 Moens, L. and Jakubowski, N. (1998) Double-focusing mass spectrometers in ICPMS. *Anal. Chem.*, **70** (7), 251A–256A.

9 Du, Z.H., Olney, T.N., and Douglas, D.J. (1997) Inductively coupled plasma mass spectrometry with a quadrupole mass filter operated in the third stability region. *J. Am. Soc. Mass Spectrom.*, **8** (12), 1230–1236.

10 Ying, J.F. and Douglas, D.J. (1996) High resolution inductively coupled plasma

mass spectra with a quadrupole mass filter. *Rapid Commun. Mass Spectrom.*, **10** (6), 649–652.

11 Winger, B.E., Lightwahl, K.J., Loo, R.R.O., Udseth, H.R., and Smith, R.D. (1993) Observation and implications of high mass-to-charge ratio ions from electrospray-ionization mass-spectrometry. *J. Am. Soc. Mass Spectrom.*, **4** (7), 536–545.

12 Lightwahl, K.J., Winger, B.E., and Smith, R.D. (1993) Observation of the multimeric forms of concanavalin-A by electrospray-ionization mass-spectrometry. *J. Am. Chem. Soc.*, **115** (13), 5869–5870.

13 Lightwahl, K.J., Schwartz, B.L., and Smith, R.D. (1994) Observation of the noncovalent quaternary associations of proteins by electrospray-ionization mass-spectrometry. *J. Am. Chem. Soc.*, **116** (12), 5271–5278.

14 Collings, B.A. and Douglas, D.J. (1997) An extended mass range quadrupole for electrospray mass spectrometry. *Int. J. Mass Spectrom. Ion. Process*, **162** (1–3), 121–127.

15 Kaiser, R.E., Cooks, R.G., Stafford, G.C., Syka, J.E.P., and Hemberger, P.H. (1991) Operation of a quadrupole ion trap mass-spectrometer to achieve high mass charge ratios. *Int. J. Mass Spectrom. Ion. Process*, **106**, 79–115.

16 Stephenson, J.L. and McLuckey, S.A. (1996) Ion/ion proton transfer reactions for protein mixture analysis. *Anal. Chem.*, **68** (22), 4026–4032.

17 Schwartz, J.C., Syka, J.E.P., and Jardine, I. (1991) High-resolution on a quadrupole ion trap mass-spectrometer. *J. Am. Soc. Mass Spectrom.*, **2** (3), 198–204.

18 Duckworth, D.C., Barshick, C.M., Smith, D.H., and McLuckey, S.A. (1994) Dynamic-range extension in glow-discharge quadrupole ion-trap mass-spectrometry. *Anal. Chem.*, **66** (1), 92–98.

19 March, R.E. and Hughes, R.J. (1989) BT Quadrupole Storage Mass Spectrometry, John Wiley and Sons, New York.

20 Garrett, A.W., Hemberger, P.H., and Nogar, N.S. (1995) Selective ionization for elemental analysis with an ion trap mass spectrometer. *Spectrochimica Acta Part B*, **50** (14), 1889–1895.

21 Eiden, G.C., Barinaga, C.J., and Koppenaal, D.W. (1996) Plasma source ion trap mass spectrometry: Enhanced abundance sensitivity by resonant ejection of atomic ions. *J. Am. Soc. Mass Spectrom.*, **7** (11), 1161–1171.

22 Schwartz, J.C., Senko, M.W., and Syka, J.E.P. (2002) A two-dimensional quadrupole ion trap mass spectrometer. *J. Am. Soc. Mass Spectrom.*, **13** (6), 659–669.

23 Hager, J.W. (2002) A new linear ion trap mass spectrometer. *Rapid Commun. Mass Spectrom.*, **16** (6), 512–526.

24 Douglas, D.J., Frank, A.J., and Mao, D.M. (2005) Linear ion traps in mass spectrometry. *Mass Spectrom. Rev.*, **24** (1), 1–29.

25 Karas, M. and Kruger, R. (2003) Ion formation in MALDI: The cluster ionization mechanism. *Chem. Rev.*, **103** (2), 427–439.

26 Mamyrin, B.A., Karataev, V.I., Shmikk, D.V., and Zagulin, V.A. (1973) Mass-reflectron a new nonmagnetic time-of-flight high-resolution mass-spectrometer. *Zhurnal Eksperimentalnoi Teoreticheskoi Fiziki*, **64** (1), 82–89.

27 Vestal, M.L., Juhasz, P., and Martin, S.A. (1995) Delayed extraction matrix-assisted laser-desorption time-of-flight mass-spectrometry. *Rapid Commun. Mass Spectrom.*, **9** (11), 1044–1050.

28 Brown, R.S. and Lennon, J.J. (1995) Mass resolution improvement by incorporation of pulsed ion extraction in a matrix-assisted laser-desorption ionization linear time-of-flight mass-spectrometer. *Anal. Chem.*, **67** (13), 1998–2003.

29 Colby, S.M., King, T.B., and Reilly, J.P. (1994) Improving the resolution of matrix-assisted laser desorption/ionization time-of-flight mass-spectrometry by exploiting the correlation between ion position and velocity. *Rapid Commun. Mass Spectrom.*, **8** (11), 865–868.

30 Dawson, J.H.J. and Guilhaus, M. (1989) Orthogonal-acceleration time-of-flight mass spectrometer. *Rapid Commun. Mass Spectrom.*, **3** (5), 155–159.

31 Myers, D.P., Mahoney, P.P., Li, G., and Hieftje, G.M. (1995) Isotope ratios and abundance sensitivity obtained with an inductively-coupled plasma-time-of-flight

mass-spectrometer. *J. Am. Soc. Mass Spectrom.*, **6** (10), 920–927.
32 Aksenov, A.A. and Bier, M.E. (2008) The analysis of polystyrene and polystyrene aggregates into the mega Dalton mass range by cryodetection MALDI TOF MS. *J. Am. Soc. Mass Spectrom.*, **19** (2), 219–230.
33 Comisarow, M.B. and Marshall, A.G. (1974) Fourier-transform ion-cyclotron resonance spectroscopy. *Chem. Phys. Lett.*, **25** (2), 282–283.
34 Zhang, L.K., Rempel, D., Pramanik, B.N., and Gross, M.L. (2005) Accurate mass measurements by Fourier transform mass spectrometry. *Mass Spectrom. Rev.*, **24** (2), 286–309.
35 Makarov, A. (2000) Electrostatic axially harmonic orbital trapping: a high-performance technique of mass analysis. *Anal. Chem.*, **72** (6), 1156–1162.
36 Hu, Q., Noll, R.J., Li, H., Makarov, A., Hardman, M., and Cooks, R.G. (2005) The Orbitrap: A new mass spectrometer. *J. Mass Spectrom.*, **40** (4), 430–443.
37 Makarov, A., Denisov, E., Kholomeev, A., Baischun, W., Lange, O., Strupat, K., and Horning, S. (2006) Performance evaluation of a hybrid linear ion trap/Orbitrap mass spectrometer. *Anal. Chem.*, **78** (7), 2113–2120.
38 Hardman, M. and Makarov, A.A. (2003) Interfacing the orbitrap mass analyser to an electrospray ion source. *Anal. Chem.*, **75** (7), 1699–1705.
39 Perry, R.H., Cooks, R.G., and Noll, R.J. (2008) Orbitrap mass spectrometry: Instrumentation, ion motion and applications. *Mass Spectrom. Rev.*, **27** (6), 661–699.
40 Weidner, S.M. and Trimpin, S. (2008) Mass spectrometry of synthetic polymers. *Anal. Chem.*, **80** (12), 4349–4361.
41 Crecelius, A.C., Baumgaertel, A., and Schubert, U.S. (2009) Tandem mass spectrometry of synthetic polymers. *J. Mass Spectrom.*, **44** (9), 1277–1286.
42 McLuckey, S.A. (1992) Principles of collisional activation in analytical mass-spectrometry. *J. Am. Soc. Mass Spectrom.*, **3** (6), 599–614.
43 Blanksby, S.J. and Mitchell, T.W. (2010) Advances in mass spectrometry for lipidomics. *Ann. Rev. Anal. Chem.*, **3**, 433–465.
44 Kondrat, R.W. and Cooks, R.G. (1978) Direct analysis of mixtures by mass-spectrometry. *Anal. Chem.*, **50** (1), 81A–92A.
45 Yost, R.A. and Enke, C.G. (1978) Selected ion fragmentation with a tandem quadrupole mass-spectrometer. *J. Am. Chem. Soc.*, **100** (7), 2274–2275.
46 Glish, G.L. and Goeringer, D.E. (1984) Tandem quadrupole-time-of-flight instrument for mass-spectrometry mass-spectrometry. *Anal. Chem.*, **56** (13), 2291–2295.
47 Glish, G.L. and Burinsky, D.J. (2008) Hybrid mass spectrometers for tandem mass spectrometry. *J. Am. Soc. Mass Spectrom.*, **19** (2), 161–172.
48 McLuckey, S.A. and Goeringer, D.E. (1997) Slow heating methods in tandem mass spectrometry. *J. Mass Spectrom.*, **32** (5), 461–474.
49 Gies, A.P., Vergne, M.J., Orndorff, R.L., and Hercules, D.M. (2007) MALDI-TOF/TOF CID study of polystyrene fragmentation reactions. *Macromolecules*, **40** (21), 7493–7504.